NOAA-20 VIIRS On-orbit Performance, Data quality, and Operational Cal/Val Support

Changyong Cao[1], Slawomir Blonski[2], Wenhui Wang[2],
Sirish Uprety[3], Xi Shao[3], Jason Choi[2], Erin Lynch[3], and Satya Kalluri[1]
[1]NOAA/NESDIS/STAR, 5830 University Research Ct., College Park, MD, 20740, U.S.A
[2]Earth Resources Tech. Inc. 14401 Sweitzer Lane Suite 300 Laurel, MD 20707 U.S.A
[3]University of Maryland, CICS, College Park, MD 20740 U.S.A

ABSTRACT

The NOAA-20 (aka JPSS-1) satellite was successfully launched on November 18, 2017 as the first in the JPSS satellite series, and a follow-on to the Suomi NPP satellite mission. The Visible Infrared Imaging Radiometer Suite (VIIRS) on-board is a major Earth observing instrument with 22 spectral bands covering the 0.41um to 12.5 um spectral range with spatial resolutions of 375 and 750 meters for the imaging and radiometric bands respectively. Since the VIIRS nadir and cryocooler doors were opened on December 13, 2017, and January 3, 2018 respectively, the instrument has been performing well and producing high quality data. The VIIRS Sensor Data Record (SDR) team has been supporting the postlaunch tests and extensive calibration/validation to ensure radiometric, spectral, and spatial performance.

This paper provides a comprehensive summary of the studies in the postlaunch calibration/validation activities which enables the VIIRS SDR to reach beta, provisional, and calibrated/validation product maturity. The instrument performance is quantified through a large number of tests involving onboard, maneuvers, as well as vicarious calibration/validation. Several issues found in the ground processing are addressed through updating the calibration input parameters known as the lookup tables (LUTs). Instrument performance waivers including the non-standard aggregation mode for the Day/Night band (DNB) and related features are addressed. On-orbit anomalies and mitigations such as the longwave infrared band degradation and saturation in some bands are also discussed. With a local equator crossing time of ~1:30pm with ~50.5 min separation from Suomi NPP achieved since January 2, 2018, NOAA-20 VIIRS provides important Earth observations for generating more than 26 global environmental data records including clouds, sea surface temperature, polar wind, aerosol, vegetation fraction, ocean color, fire, snow and ice for weather, and other environmental applications.

Keywords: NOAA-20, VIIRS, on-orbit performance, calibration/validation

1. INTRODUCTION

The NOAA-20 (also known as JPSS J1) was launched on November 18th, 2017 with four major Earth observing instruments including the Visible Infrared Imaging Radiometer Suite (VIIRS), Cross-track infrared Sounder (CrIS), Advance Technology Microwave Sounder (ATMS), and Ozone Mapping Profiler Suite (OMPS) for weather applications and environment monitoring. The VIIRS on-board is a major Earth observing instrument with 22 spectral bands covering the 0.41um to 12.5 um spectral range with spatial resolutions of 375 and 750 meters for the imaging and radiometric bands respectively. Since the VIIRS nadir and cryocooler doors were opened on December 13, 2017, and January 3, 2018 respectively, the instrument has been performing well and producing high quality data. The VIIRS Sensor Data Record (SDR) team has been supporting the postlaunch tests and extensive calibration/validation to ensure its radiometric, spectral, and spatial performance. With a local equator crossing time of ~1:30pm with ~50.5 min separation from Suomi NPP achieved since January 2, 2018, NOAA-20 VIIRS provides important Earth observations for generating more than 26 global environmental data records including clouds, sea surface temperature, polar wind, aerosol, vegetation fraction, ocean color, fire, snow and ice for weather, climate, and other environmental applications. This paper provides a comprehensive summary of the results in the postlaunch calibration/validation which enables the VIIRS SDR to reach beta, provisional, and calibrated/validation product maturity. The instrument performance is quantified through a large number of tests involving onboard, maneuvers, as well as vicarious calibration/validation. Several issues found in the

Earth Observing Missions and Sensors: Development, Implementation, and Characterization V
edited by Xiaoxiong Xiong, Toshiyoshi Kimura, Proc. of SPIE Vol. 10781, 107810K
 · doi: 10.1117/12.2324329

ground processing are addressed through updating the calibration input parameters known as the lookup tables (LUTs). Instrument performance waivers including the non-standard aggregation mode for the Day/Night band (DNB) and related features are addressed. On-orbit anomalies and mitigations such as the longwave infrared band degradation and saturation in some bands are also discussed. The radiometric biases between NOAA-20 VIIRS and other radiometers are quantified using a number of techniques. In the following sections, after reviewing the postlaunch tasks and timelines, we present the NOAA-20 VIIRS features and performance. Then the known issues and mitigations are discussed and a summary is provided.

2. NOAA-20 VIIRS ON-ORBIT CALIBRATION/VALIDATION TASKS

Based on experience gained from the Suomi NPP VIIRS calibration/validation [1], a plan has been developed for the NOAA-20 VIIRS postlaunch cal/val. The plan is based on a set of tasks supported by an expert team from several organizations, including NOAA, NASA, The Aerospace Corp., University of Wisconsin, and University of Maryland/CICS. The previous list of tasks used for Suomi NPP [1] has been revised for NOAA-20 VIIRS. Table 1 shows the tasks aligned with the postlaunch milestones. For example, after launch but before the nadir door open (launch + 10 days), a number of tests were performed to check the ephemeris and attitude data, scan data, detector noise, DC restore, DNB straylight, SD and SDSM characterization, as well as blackbody temperature uniformity. After the nadir door opened on L+24, additional tests were performed for the reflective solar bands to verify aggregation, bow-tie deletion, image quality, dynamic range, response vs. scan, geolocation, and comparisons with MODIS and SNPP VIIRS. By launch + 45 days, the cryo-radiator door was opened to activate the thermal emissive bands (TEB). The cal/val tasks included crosstalk evaluation, comparison with CrIS, lunar calibration, pitch maneuver data analysis, and DNB straylight correction. Additional tests were performed before the validated maturity was reached, which included radiometric bias evaluation, band to band co-registration, update of the calibration parameters in the lookup tables (LUTs).

Table 1. NOAA-20 VIIRS Postlaunch Cal/Val Tasks

Task ID	Task
	Instrument Activation (L+10)
GEO-1	Initial Validation of Spacecraft Ephemeris and Attitude Data
GEO-2	Initial Validation of VIIRS Encoder Data, Scan Time, Scan Period, and Scan Rate
FPF-2	Detector Operability and Noise Verification with Nadir Door Closed: RSB VNIR,
FPF-6	DC-Restore Functionality and Performance Check
FPF-7	Calibrator Visual Inspection
PLT-X	DNB Straylight with Nadir Doors Closed (using sector rotation)
CSE-1	SD and SDSM Characterization
CSE-2	Onboard Calibrator Black Body (OBCBB) Temperature Uniformity
CSE-4	Temporal Analysis of SD Signal over Polar Region
CSE-5	Temporal Analysis of Solar Diffuser Stability Monitor (SDSM) Data
PTT-1	Operability, Noise, SNR Verification
PTT-6	Telemetry Trending Monitoring
PTT-10	RSBAutoCal Calibration Object Trending, Evaluation & LUT Updates
RAD-24	Offline F/H Factor Analysis, Prediction and Validation Tool
	Nadir Doors Open (L+24)
FPF-3	In-Scan Aggregation Verification – non-DNB bands
FPF-4	Dual Gain Band and DNB Transition Verification
FPF-5	On-Board Bow-Tie Deletion Verification
CSE-3	Earthshine Contamination of Solar Diffuser Data
IMG-1	Crosstalk, Echo, and Ghost Investigation
IMG-2	Image Analysis (Striping, Glints and Other Artifacts)
RAD-3	Dynamic Range and Linearity
RAD-4	Response vs. Scan Angle (RVS)
RAD-7	SDR Comparison with SNPP-VIIRS
RAD-8	SDR Comparison with MODIS
RAD-8'	SDR Comparison with AVHRR
GEO-3	Assess Reasonableness of First- Period SDR Geolocation
GEO-4 to 7	Analyze First-Period VIIRS GCP Residuals
GEO-9	Develop and Test Initial Geolocation LUT Updates
PTT-2	RDR Histogram Analysis
WAV-1	J1 DNB aggregation mode verification
WAV-2	J1 DNB geolocation vs. aggregation zone

Task ID	Task
	Cryo-radiator Door Open (L+45)
IMG-3	Moon Echo and Ghost Check
CSE-6	Yaw Maneuver Analysis
RAD-1	Out-of-Band (OOB) Spectral Leakage
RAD-2	Crosstalk from Emissive Bands to Reflective Bands
RAD-6	SDR Comparison with Model
RAD-9	RSB Radiance/Reflectance Validation – Radiometric Sites
RAD-10	Brightness Temperature Validation Using Buoy Data
RAD-11	In-Band Spectral Radiance Comparison with CrIS
RAD-14	Emissive Band Response Characterization (WUCD)
RAD-15	Moon in Space View Correction
RAD-18	Lunar Data Analysis - Roll Maneuver
RAD-19	Analysis of Pitch Maneuver Data
RAD-20	SDR Reprocessing and Updates
RAD-23	Dual Gain Band Anomaly Analysis
PTT-4	DNB Offset Verification
WAV-4	J1 DNB straylight assessment and correction LUT development
	Validated Maturity (L+180)
PLT	DNB SIMULTANEOUS LGS/MGS/HGS-A/B IMAGES OVER SAA
IMG-4	LSF/MTF VALIDATION
RAD-5	RELATIVE BAND-TO-BAND CALIBRATION ANALYSIS USING LUNAR DATA
RAD-12	Band-to-Band Radiometric Comparison
RAD-13	Structured Scene Analysis
RAD-16	RSB Radiance/Reflectance Validation – Underflights & Field
RAD-17	Spectral Validation Using Hyperspectral Data from Aircraft
RAD-21	Radiometric Calibration Validation with GIRO
RAD-22	Radiometric Calibration Validation with Lunar Band Ratio
RAD-25	Radiometric Model Development & On-Orbit Update
GEO-8	ANALYZE INITIAL INTRA-ORBIT THERMAL EFFECTS ON GEOLOCATION
GEO-10	Band-to-Band Registration using the Moon
GEO-11	Band-to-Band Registration (BBR) Verification
GEO-12	Band-to-Band Registration using ground targets
GEO-13	LSF/MTF Validation
GEO-14	LSF/MTF Estimation using the Moon
PTT-7	Update Uploadable Tables ID5, ID33-35: DNB Offsets
PTT-8	Update Uploadable Table ID4: DNB Radiation Thresholds
WAV-5	J1 DNB radiometric/geolocation monitoring using point sources
WAV-6	J1 VIIRS saturation monitoring
WAV-8	J1 VIIRS polarization characterization

The postlaunch cal/val of NOAA-20 VIIRS progressed well as planned. Figure 2 shows the major milestones, and events since NOAA-20 launch, upto August 2018. The green labels in the figure show major milestones which include the beta, provisional, and validated maturity, as well as the turn-over to operations. The blue labels denote ground processing algorithm and lookup table changes based on analysis from postlaunch data to improve the data quality. Red labels show the flight project related activities, including maneuvers, lunar calibration, outgassing, and orbit raising. Finally, as is indicated in gray on the lower section of the timeline, NOAA-20 VIIRS still suffers occasional sync loss between the rotating telescope and the half angle mirror. When the sync loss occurs, about two minutes of data are lost and this happens approximately every two weeks. It is expected that the instrument vendor will further investigate the root cause of the sync loss and fix it for future models.

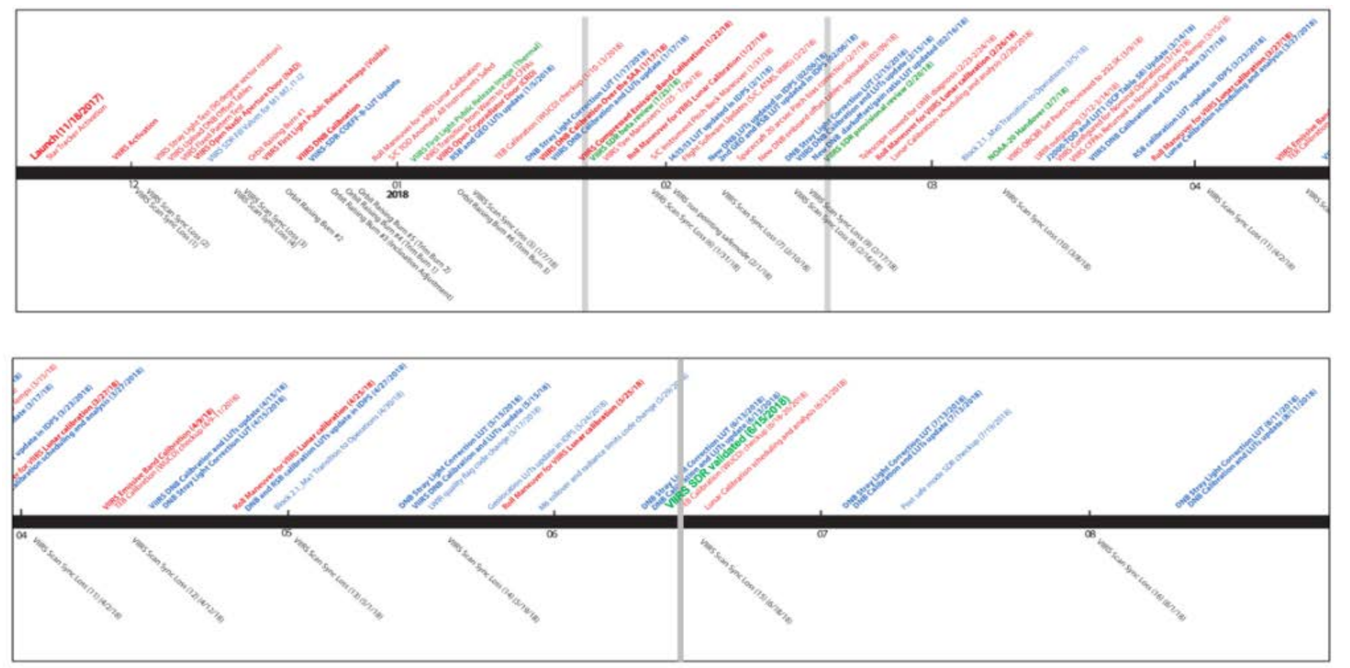

Figure 2. NOAA-20 VIIRS Postlaunch Events.

3. NOAA-20 VIIRS FEATURES AND PERFORMANCE

The VIIRS instrument design has been well-characterized in previous studies. Although NOAA-20 VIIRS shares the same design as that of the Suomi NPP, there are minor differences. These differences are due to deviations in making the instrument. For example, the spectral response functions of the VIIRS bands are slightly different between NOAA-20 and Suomi NPP VIIRS. Another major difference is the VIIRS DNB aggregation mode. For Suomi NPP, the typical 32 aggregation zones across scan are used. However, for NOAA-20, due to noise and nonlinearity issues in high aggregation zones, the high aggregation zones above zone 21 use the same aggregation scheme of zone 21, which leads to non-typical DNB images, and also allows for more data at the edge of the scan[2]. Nevertheless, VIIRS on NOAA-20 is a near identical copy of the one on Suomi NPP. Figure 3 shows the first light image of VIIRS true color composite from bands M5, M4, and M3 as RGB. It captured a major California fire, smoke, and plum at the time.

Figure 3. NOAA-20 VIIRS First Light Image Acquired on December 13, 2017

Among the many instrument specifications, instrument noise, as in the signal to noise ratio (SNR) for the reflective solar bands (RSB) and noise equivalent delta temperature (NEDT) for the thermal emissive bands (TEB), is a major requirement for instrument performance. Based on extensive postlaunch analysis, it was found that the noise performance of VIIRS on NOAA-20 is comparable to the VIIRS on Suomi NPP. Figure 4 provides comparisons between the two instruments for all bands. For the RSB, the NOAA-20 VIIRS SNRs are slightly better than those for Suomi NPP, and both VIIRS on NOAA-20 and Suomi NPP perform better than the specification (as shown in red). Note that band I3 has a dead detector which causes striping. As a result, the SNR calculations excluded the dead detector. For the TEB, the NEDT for all bands are comparable between Suomi NPP and NOAA-20 VIIRS, and they all perform better than the specifications. For the DNB, the SNRs are significantly better than the specification. However, NOAA-20 has 21 aggregation modes as compared to the 32 aggregation modes for Suomi NPP VIIRS. Also, the SNRs for DNB are calculated using blackbody radiance, which is at the minimum detectable radiance of 3 nW/cm^2-sr and at the same level as the specification for Suomi NPP VIIRS SNR. However, for NOAA-20 VIIRS DNB, the blackbody radiance for the DNB is only 2nW/cm^2-sr, which led to the differences in the SNR between these two in the figure. In other words, if the NOAA-20 VIIRS DNB SNR is normalized to the specification of 3 nW/cm^2-sr, the NOAA-20 VIIRS DNB SNR would be higher than that of the Suomi NPP VIIRS.

Band	L_typ	SNR Spec	NOAA-20 (on-orbit)	S-NPP (on-orbit)
M1 LG	155	316	1115	1045
M1 HG	44.9	352	644	588
M2 LG	146	409	1012	1010
M2 HG	40	380	573	572
M3 LG	123	414	1057	988
M3 HG	32	416	686	628
M4 LG	90	315	857	856
M4 HG	21	362	551	534
M5 LG	68	360	762	631
M5 HG	10	242	383	336
M6	9.6	199	413	368
M7 LG	33.4	340	708	631
M7 HG	6.4	215	523	457
M8	5.4	74	319	221
M9	6	83	297	227
M10	7.3	342	653	586
M11	1	90	198	22*
I1	22	119	224	214
I2	25	150	285	264
I3	7.3	6	174	149

Band	T_typ	NEDT Spec	NOAA-20 (on-orbit)	S-NPP (on-orbit)
M12	270	0.396	0.12	0.12
M13	300	0.107	0.04	0.04
M14	270	0.091	0.05	0.06
M15	300	0.07	0.02	0.03
M16	300	0.072	0.03	0.03
I4	270	2.5	0.42	0.4
I5	210	1.5	0.42	0.4

Band	L_min	SNR Spec	NOAA-20 (on-orbit)	S-NPP (on-orbit)
DNB**	3	6	>10	>10

* For S-NPP M11, L_{typ} = 0.12 W/m^2-sr-μm

** On-orbit SNR of DNB at L_{min} was evaluated by using the DNB OBC-BB data

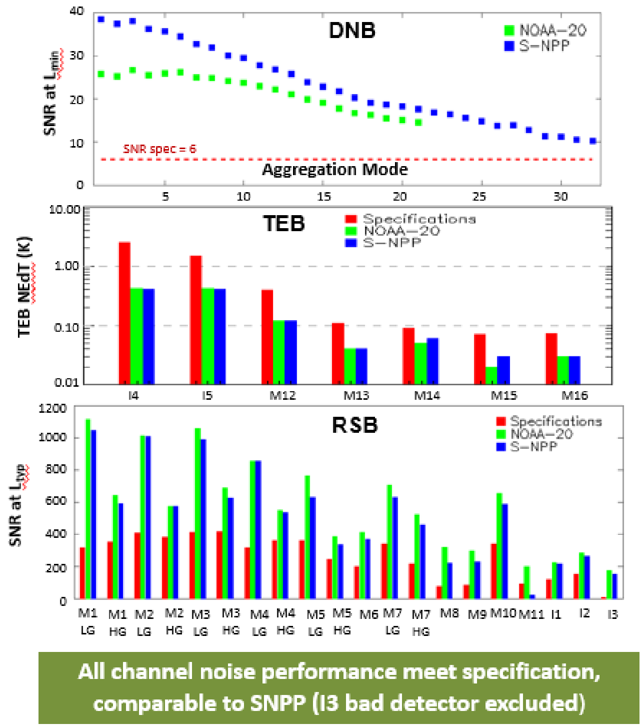

Figure 4. NOAA-20 VIIRS Noise Performance

4. NOAA-20 VIIRS KNOWN ISSUES AND MITIGATIONS

4.1 NOAA-20/VIIRS DNB Aggregation Mode 21

The unique feature of NOAA-20 VIIRS/DNB aggregation mode has been fully discussed in another paper [2]. Here only a brief summary is provided. By design, the VIIRS/DNB has 32 aggregation zones from nadir to end of scan. This is necessary to provide a constant spatial resolution of 750m over the entire scan range, as opposed to the increasing pixel size with scan angle seen in nearly all other remote sensing instruments. This 32 aggregation zone was used for Suomi NPP VIIRS successfully and it works well. However, for NOAA-20 VIIRS/DNB, it was found in prelaunch tests that there is high nonlinearity at high scan angles (above aggregation zone 21), which would introduce large noise if the original 32 aggregation zone were used. As a result, the alternative aggregation method of applying the same aggregation 21 scheme to the high scan angles (starting from agg21 and ending at agg32) mitigates this issue. This led to the non-typical aggregation of DNB on NOAA-20. This also allowed more samples at the end of the scan to be included in the SDR data (extended region). This change required software and LUT modifications which have been tested both prelaunch and postlaunch.

4.2 Initial Production of VIIRS SDR data

When the NOAA-20 VIIRS nadir door was opened on December 13, 2017, the data processing system IDPS was having difficulties in producing the first light image. An investigation revealed that this was due to lower than expected instrument component temperatures which the calibration algorithms use in conjunction with the LUTs. Test data were produced offline to generate the first light image. This issue was fixed by updating the LUTs in the IDPS.

4.3 Unexpected Longwave Infrared Channel Responsivity Degradation

Soon after the cryo-radiator door was opened on January 3, 2018 and the TEB bands started producing data, it was found that the longwave infrared bands have a larger than expected degradation in the responsivity on the order of 0.1% per week. This is unusual since for most longwave infrared bands, the degradation rate is very low and it typically takes many years for it to degrade by half a percent. Intensive studies of this issue had been performed by the VIIRS SDR team, in collaboration with the NASA flight project. Based on experience from previous cal/val endeavors with satellite instruments such as GOES imager and IASI infrared sounder, it was hypothesized that water vapor accumulation in the aft optics may be the culprit of the longwave degradation. This is further confirmed by the differential degradation rate between longwave infrared bands, since those channels with more water vapor absorption would degrade faster than the window channels. To validate this hypothesis, the flight project initiated the mid-mission outgassing, which served to warm up the aft optics in the longwave infrared to remove the water vapor. This was done on March 12-14, 2018, after which it was found that the outgassing was very successful, and the longwave infrared channel responsivity was regained (Figure 5). There is, however, a small degradation in the band I5 from April to August, 2018, but it returned to normal after an instrument reset on 7/19/2018 with a single event upset (SEU) over the SAA. It is hypothesized that the I5, being more sensitive to the water vapor buildup due to its broader spectral responses, may be sensing some residual water vapor in the aft optics and its performance will be closely monitored.

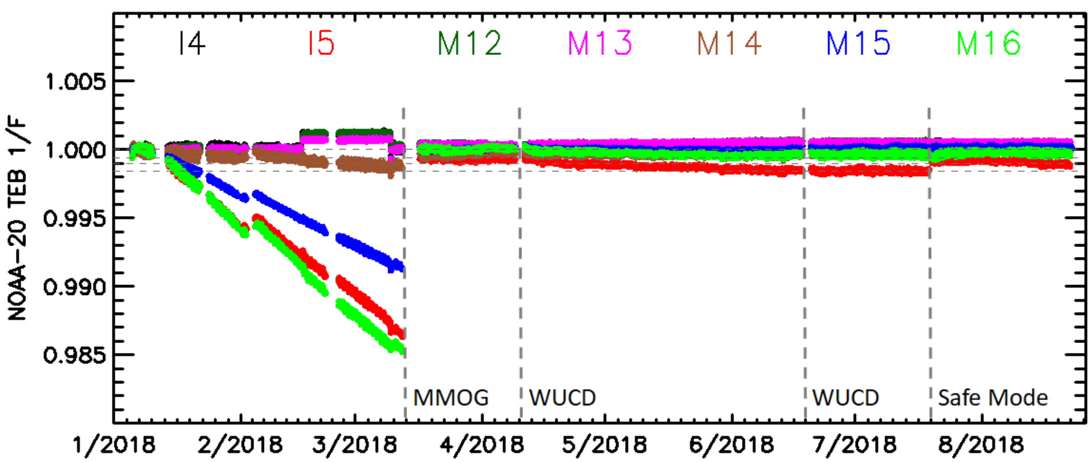

Figure 5. NOAA-20 VIIRS Longwave Infrared Channel Responsivity change before and after outgassing

4.4 Solar Diffuser Calibration Instability

The reflected solar band calibration relies on the solar diffuser, but unfortunately, the solar diffuser data, which is used to produce the H-factor, had an unexpectedly large oscillation over time (Figure 6). The oscillation is on the order of 2% peak to peak, which introduced an unallocated uncertainty in the calibration [3]. Investigation by the SDR team found that this oscillation is likely caused by uncertainties in the prelaunch Solar Diffuser Stability Monitor (SDSM) Sun view transmittance function [3] [4]. To resolve this issue, ideally, more yaw maneuvers would be executed in order to characterize the solar diffuser reflectance at various angles. However, this is difficult, time consuming, and costly. As a result, the VIIRS SDR team developed a correction procedure to mitigate this effect using yaw and on-orbit SDSM data together [4]. After the SDSM detector correction [4], the solar diffuser degradation trend becomes much more smooth as expected (Figure 6). It is expected that this solar diffuser BRF model can be further improved with more SDSM data collected over a large range of solar azimuth angles over a year or longer.

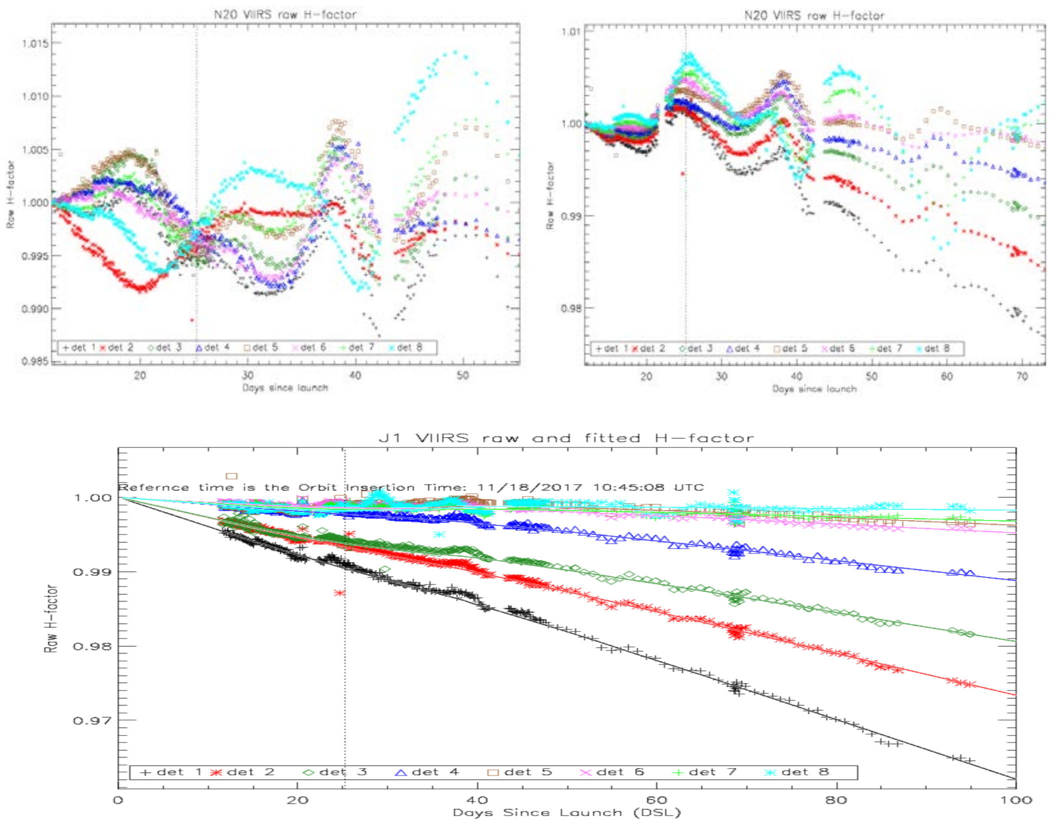

Figure 6. Solar Diffuser Calibration Stability Improvement before and after correction (upper left - H-factor using prelaunch LUT; upper right- H-factor using yaw derived LUT; lower: H-factor using yaw and on-orbit SDSM data with gain correction)

4.5 RSB Radiometric Bias

Major efforts have been devoted to the quantification of radiometric biases between VIIRS on NOAA-20, Suomi NPP, and MODIS. In the postlaunch radiometric intercomparisons using various methods including SNO over polar regions, extended SNO (SNOx) over the Saharan desert and tropical ocean, deep convective clouds, and intercomparison with Landsat 8 OLI,, it was found that after the initial check out period and all LUTs were updated, there is a consistent bias between Suomi NPP and NOAA-20 VIIRS reflective solar bands. Figure 7 shows bias for a few bands over desert using SNOx. Results show that NOAA-20 VIIRS is consistently biased lower than those equivalent bands on Suomi NPP. After subtracting this 2% bias, NOAA-20 and Suomi NPP VIIRS are in good agreement for most channels. Exceptions are bands M5 and M7, where a residual bias on the order of 1-2% still exists. However, this positive bias for M5 and M7 is expected based on previous studies because it was found during the Suomi NPP cal/val that these two bands are too high in their radiometric values when compared to MODIS, even after accounting for the spectral response differences.

The root cause of the radiometric biases for NOAA-20 VIIRS is currently being investigated. Early results show that it is most likely caused by prelaunch characterization uncertainties in the solar diffuser. Although both Suomi NPP and NOAA-20 VIIRS meet the specification in prelaunch tests, these two may have biases in opposite directions which leads to large biases between them. It is noted that the NOAA-20 reflective solar band calibration uses the Thuillier solar spectrum[5], while that for Suomi NPP uses the solar spectrum from MODTRAN4. However, it is known that this difference does not cause biases when the intercomparison is performed in reflectance instead of radiance [6].

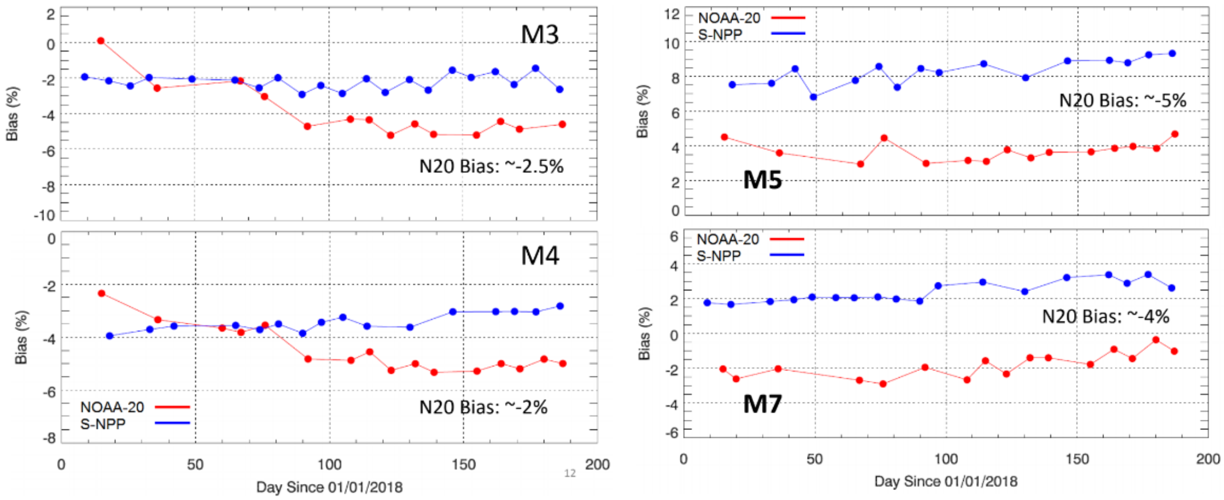

Figure 7. Reflectance bias between VIIRS on NOAA-20 and Suomi NPP at the SNOx (using MODIS as reference for double difference)

4.6 Other Issues

Several other issues were also found during the NOAA-20 VIIRS cal/val. These include the TEB Scan Angle Dependent Bias when compared to collocated CrIS observations which is currently under investigation. The initial errors in geolocation have also been resolved by updating the instrument mounting matrix postlaunch. On the other hand, sync loss still exists for NOAA-20 VIIRS with similar occurrence frequencies which requires further investigation into its root cause.

5. SUMMARY

Based on extensive NOAA-20 VIIRS postlaunch cal/val, it was found that the instrument is performing well. Several performance issues have been resolved, including the longwave infrared band degradation, calibration LUT updates, and DNB straylight correction. The NOAA-20 VIIRS SDR has achieved validated maturity. Remaining issues include the constant bias between NOAA-20 and Suomi NPP, which is currently under investigation. It is expected that once the root cause is identified, a solution can be developed to resolve the bias. The VIIRS SDR team has provided dedicated support to the NOAA-20 cal/val which has enabled the data to achieve beta, provisional, and finally validated maturity. The team will continue support the NOAA-20 VIIRS and beyond in the JPSS program.

Acknowledgments

The authors would like to thank the entire VIIRS SDR team and partners for their dedicated support to the NOAA-20 postlaunch cal/val. The manuscript contents are solely the opinions of the authors and do not constitute a statement of policy, decision, or position on behalf of NOAA or the U.S. government. This study is partially funded by the NOAA Joint Polar Satellite System (JPSS) program.

REFERENCES

[1] C. Cao, F. J. De Luccia, X. Xiong, R. Wolfe, and F. Weng, "Early on-orbit performance of the visible infrared imaging radiometer suite onboard the suomi national polar-orbiting partnership (S-NPP) satellite," *IEEE Trans. Geosci. Remote Sens.*, vol. 52, no. 2, pp. 1142–1156, 2014.

[2] Wang, W., & Cao, C. (2018). "NOAA-20 VIIRS Day/Night Band Unique Feature and Preliminary Verification On-Obit". In, *2018 International Geoscience and Remote Sensing Symposium*. Valencia, Spain (July 23-27, 2018)

[3] T. Choi, S. Blonski, C. Cao, " Initial on-orbit radiometric calibration of the NOAA-20 VIIRS Reflective Solar Bands," Proc. SPIE Earth Observing Systems XXIII, Vol. 10764, 2018
[4] T. Choi, X. Shao, S. Blonski, C. Cao, "Improving NOAA 20 VIIRS screen transmittance and solar diffuser BRF estimation from both Yaw maneuver and regular on-orbit data," Proc. SPIE Sensors, Systems, and Next-Generation Satellites, Vol. 10785, 2018
[5] Thuillier, G., M. Hersé, P. C. Simon, D. Labs, H. Mandel, D. Gillotay, and T. Foujols, "The solar spectral irradiance from 200 to 2400 nm as measured by the SOLSPEC spectrometer from the ATLAS and EURECA missions," *Solar Physics*, vol. 214, no. 1, pp. 1-22, 2003.
[6] C. Cao, J. Xiong, S. Blonski, Q. Liu, *et al.*, “Suomi NPP VIIRS sensor data record verification, validation, and long-term performance monitoring,” *J. Geophys. Res. Atmos.*, vol. 118, no. 20, pp. 11664–11678, 2013.